Supporting Information

On the origin of the robust catalytic performance of nanodiamond-graphene-supported Pt nanoparticles used in the propane dehydrogenation reaction

Jie Liu,[†, ‡] Yuanyuan Yue,[†] Hongyang Liu,*[, §] Zhijian Da,[‡] Changcheng Liu,[‡] Aizeng Ma,[‡] Junfeng Rong,*[, ‡] Dangsheng Su,*[, §] Xiaojun Bao[‡] and Huidong Zheng[‡]

[†] School of Chemical Engineering, Fuzhou University, 2 Xueyuan Road, Fuzhou 350116, P. R. China.

[‡] Research Institute of Petroleum Processing, Sinopec, 18 Xueyuan Road, Beijing 100083, P. R. China.

[§] Shenyang National Laboratory for Materials Science, Institute of Metal Research, Chinese Academy of Sciences, 72 Wenhua Road, Shenyang 110016, P. R. China.

Corresponding Author:

*liuhy@imr.ac.cn

*rongjf.ripp@sinopec.com

*dssu@imr.ac.cn

Table of Contents

1. Experimental section

a) Taking the case of Pt/ND@G, the propane rate was calculated as follows:

$$\text{Propane rate}=\frac{\frac{3\times10^{-3}\times60}{22.4}\times(12.81\text{-}6.26)\%}{0.2\times0.283\%}=929.30\ \text{mmol}\ g_{P_t}^{-1}\ h^{-1}$$

where $F_{propane}$ (the flow rate of propane) = 3 mL min^{-1}; X (the conversion of propane) = (12.81-6.26)%=6.55%, 12.81% represents the conversion of propane over Pt/ND@G, 6.26% represents the conversion of propane over ND@G support, and the reaction time is 0.5 h; $m_{cat.}$ (the percentage of Pt weight loading in the catalyst) = 0.2 g; w_{p_t} = 0.283%.

b) The TOFs were calculated based on the conversion data at 30 ºC, and they were 90.5% for Pt/ND@G, 36.2% for Pt/OLC, 1.4% for Pt/AC, and 1.2% for Pt/Al_2O_3. Taking the case of Pt/ND@G, the TOF was calculated as follows:

$$\text{TOF}=\frac{\frac{15\times1\%\times60}{22.4}\times195.1\times90.5\%}{0.05\times4.22\%\times\frac{1}{1.72}}=57.8\ h^{-1}$$

where F_{CO} (the flow rate of CO) = 15×1% = 0.15 mL min^{-1}; M_{p_t} = 195.1 g mol^{-1}; X (the conversion of CO) = 90.5%; $m_{cat.}$ (the percentage of Pt weight loading in the catalyst) = 0.05 g; w_{p_t} = 4.22%; *Dis.* (the dispersity of Pt) = 1/1.72.

2. Supporting Table

Table S1. Results of Py-FTIR experiments of Pt/Al_2O_3 and Pt/ND@G.

Samples	200 ºC		350 ºC		T[a]
	L (μmol g^{-1})	B (μmol g^{-1})	L (μmol g^{-1})	B (μmol g^{-1})	L (μmol g^{-1})
Pt/Al_2O_3	2004.7	--	1270.0	--	734.7
Pt/ND@G	--	--	--	--	--

[a] T, which represents the difference between the acid amount of 200 ºC and 350 ºC, is regarded as the acid amount of the weak acids.

Note: The acid amount derived from the peak accorded at 200 ºC represents the total acidity, and the acid amount corresponding to the peak at 350 ºC indicates the amount of the medium strong acids.[1,2]

3. Supporting Figures

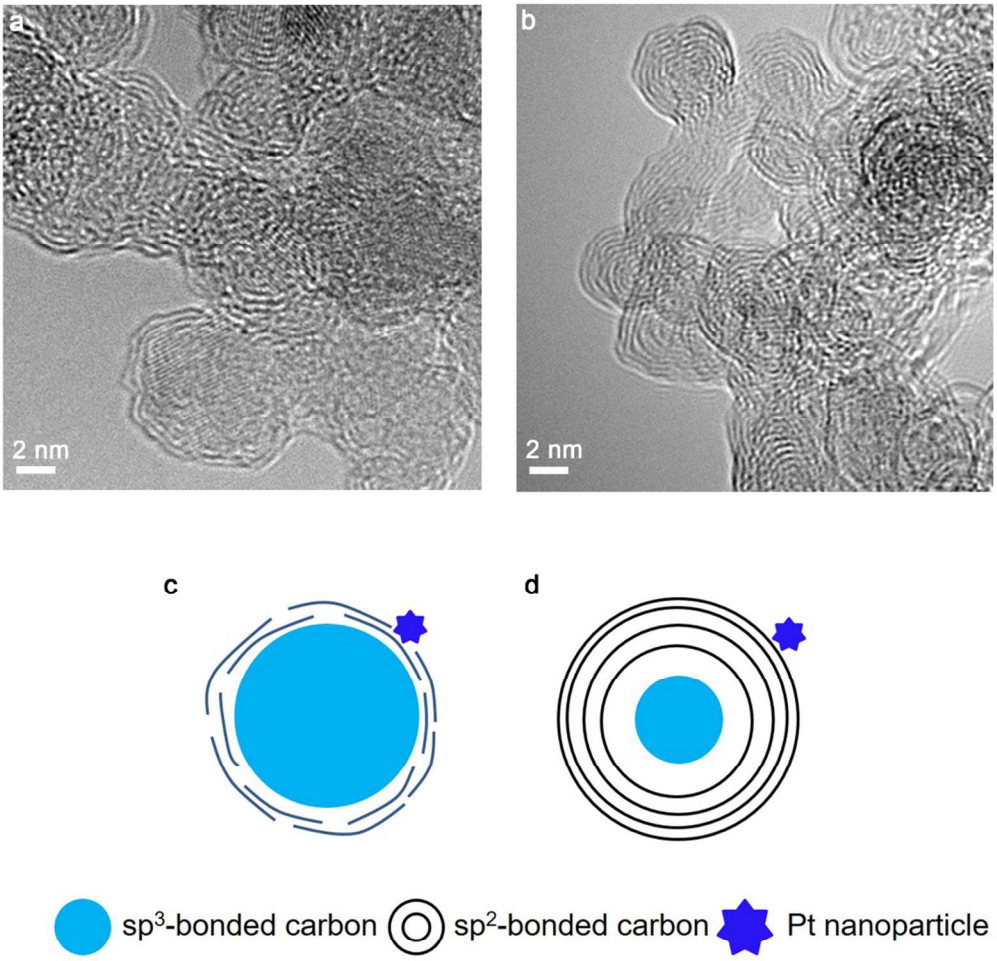

Figure S1. High-resolution TEM images and schematic drawings of (a, c) Pt/ND@G and (b, d) Pt/OLC catalysts. The theoretical Pt weight loading was 0.5 wt% for each sample.

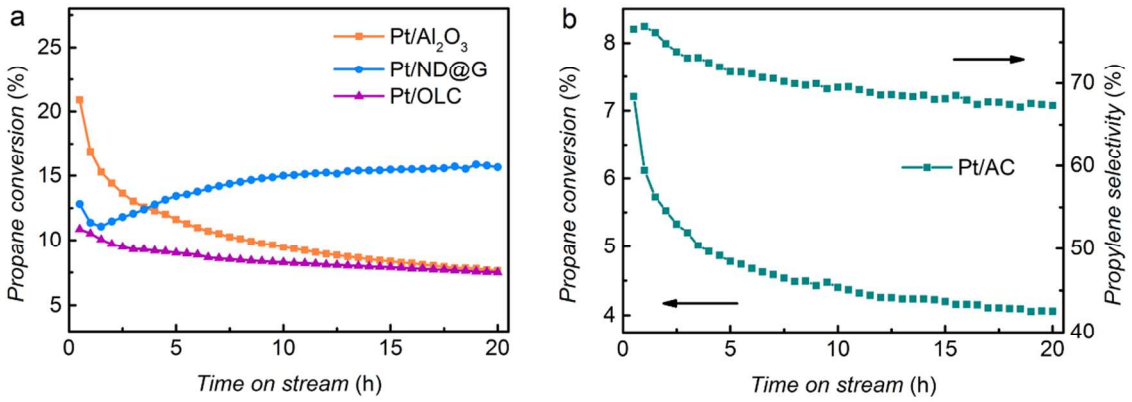

Figure S2. Catalytic activities of the (a) as-prepared catalysts and (b) commercial Pt/AC catalyst during the propane dehydrogenation reaction. The theoretical Pt weight loading for Pt/Al_2O_3 was 0.3 wt%, those for Pt/ND@ and Pt/OLC were both 0.5 wt%, and that for the commercial Pt/AC was 5 wt%.

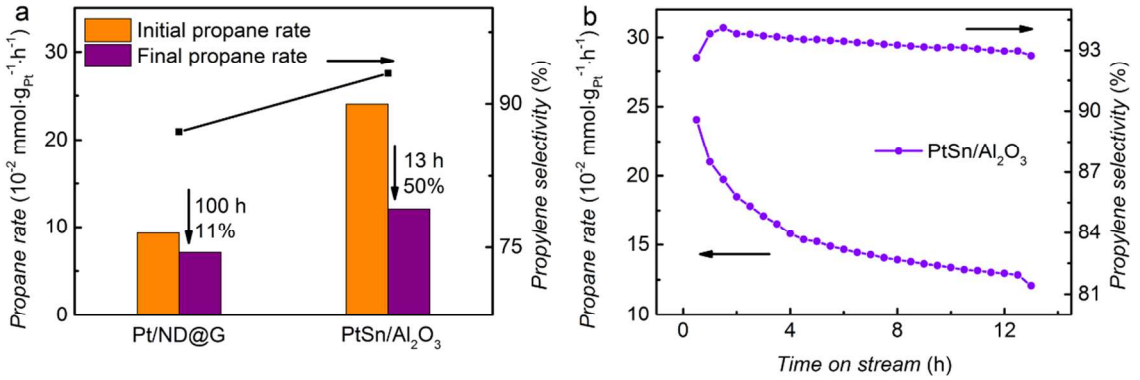

Figure S3. (a) Comparison of the catalytic performances between Pt/ND@G and $PtSn/Al_2O_3$ and (b) catalytic activities of $PtSn/Al_2O_3$ catalyst during the propane dehydrogenation reaction. The theoretical Pt and Sn weight loadings for lab-made $PtSn/Al_2O_3$ were 0.3 wt% and 0.2 wt%, respectively. The theoretical Pt weight loading for Pt/ND@G was 0.5 wt%. The propylene selectivities of the catalysts after a 10 h propane dehydrogenation reaction.

The catalytic performances of Pt/ND@G and $PtSn/Al_2O_3$ catalysts (which was prepared according to our previous work[3]) during the propane dehydrogenation (PDH) reaction are shown in Figure S3. By comparison with the monometallic Pt/ND@G catalyst, the bimetallic $PtSn/Al_2O_3$ catalyst shows higher propane rate and propylene selectivity. Generally, the addition of Sn species can increase the dispersity of Pt, improve the accessibility between propane and the active sites, inhibit the structure-sensitive side-reactions, then promote the catalytic performance;[4,5] in addition, the introduction of Sn species has influence on the electron density of Pt, changes the absorption process of propane and desorption process of propylene, thus may benefit to obtaining higher catalytic activity.[6] However, there is a sharp decrement in the propane rate for $PtSn/Al_2O_3$ catalyst than that for Pt/ND@G under the same reaction condition. For example, the propane rate of $PtSn/Al_2O_3$ decreases by 50% in the 13 h test, and the propane rate of Pt/ND@G only decreases by 11% in the 100 h test. In summary, the

result in Figure S3 confirms that Pt/ND@G catalyst possesses a remarkable stability for the high-temperature PDH reaction.

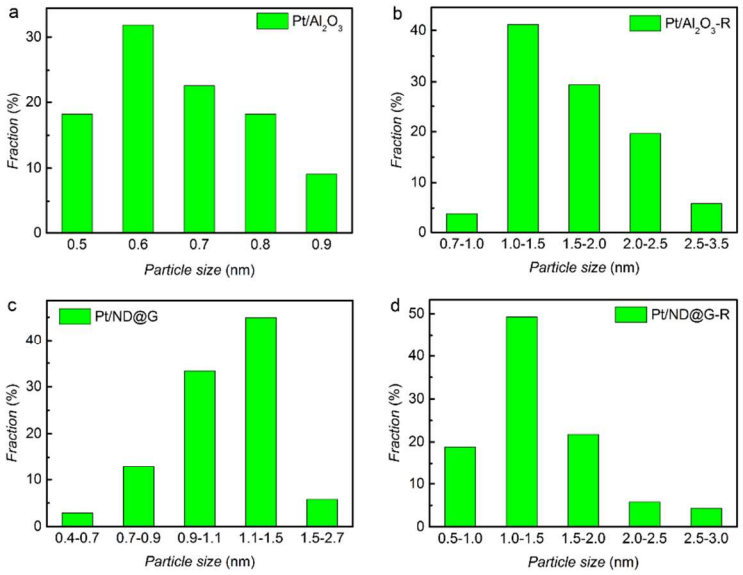

Figure S4. Pt nanoparticle size distributions of (a) Pt/Al_2O_3, (b) Pt/Al_2O_3-R, (c) Pt/ND@G and (d) Pt/ND@G-R. '-R' represents the spent catalysts. The theoretical Pt weight loading for Pt/Al_2O_3 was 0.3 wt%, and that for Pt/ND@G was 0.5 wt%.

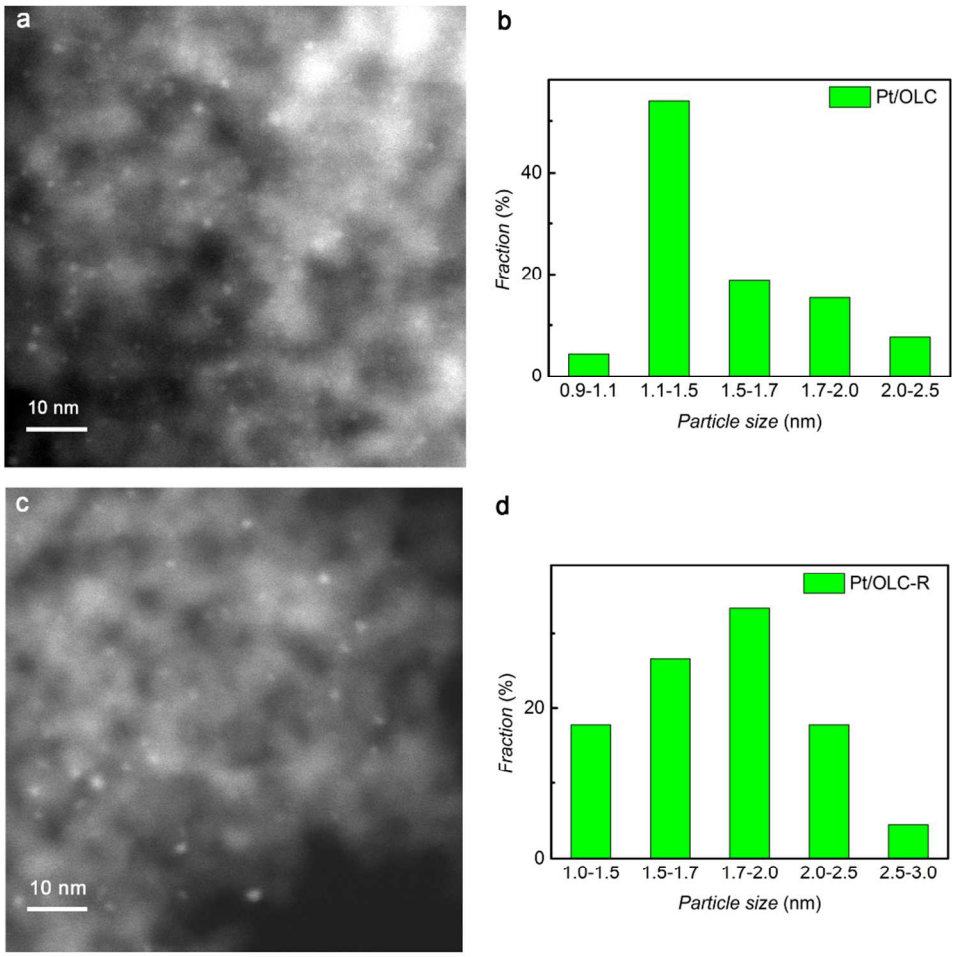

Figure S5. STEM images and Pt nanoparticle size distributions of (a, b) Pt/OLC and (c, d) Pt/OLC-R. '-R' represents the spent catalysts. The theoretical Pt weight loading for Pt/OLC was 0.5 wt%.

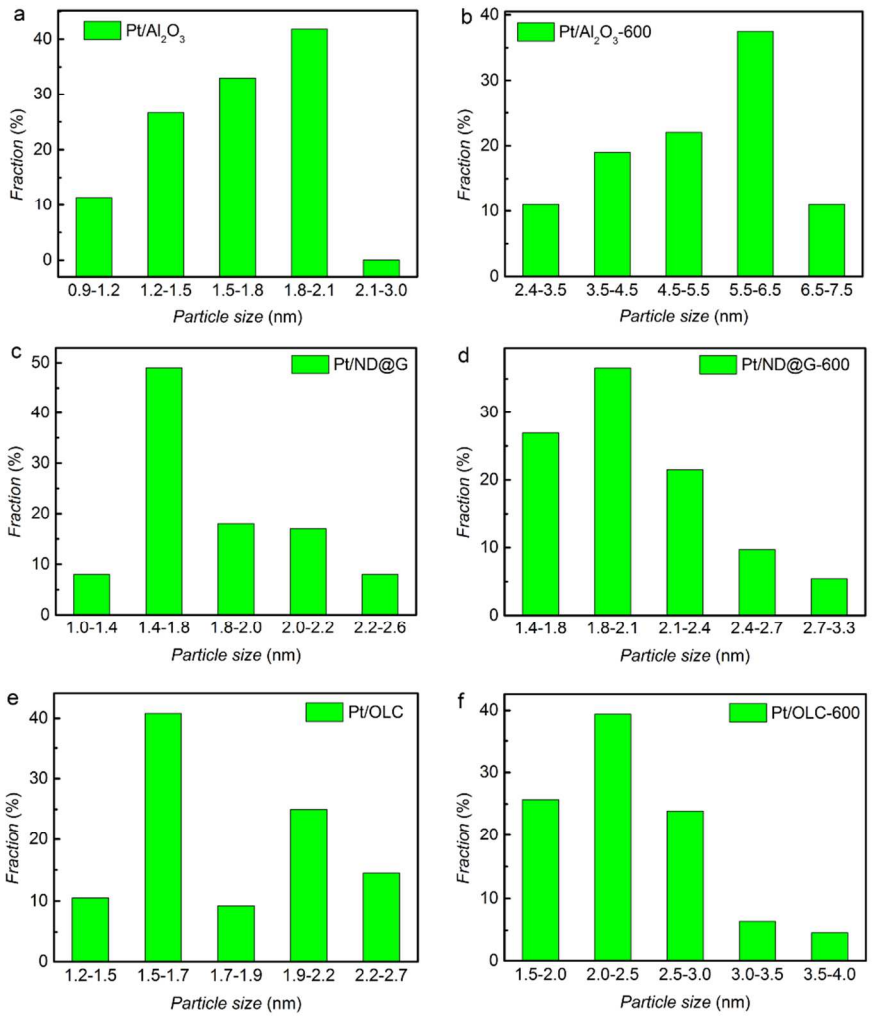

Figure S6. Pt nanoparticle size distributions of (a) Pt/Al_2O_3, (b) Pt/Al_2O_3-600, (c) Pt/ND@G, (d) Pt/ND@G-600, (e) Pt/OLC and (f) Pt/OLC-600. '-600' represents the annealed catalysts. The theoretical Pt weight loading was 5 wt% for each sample.

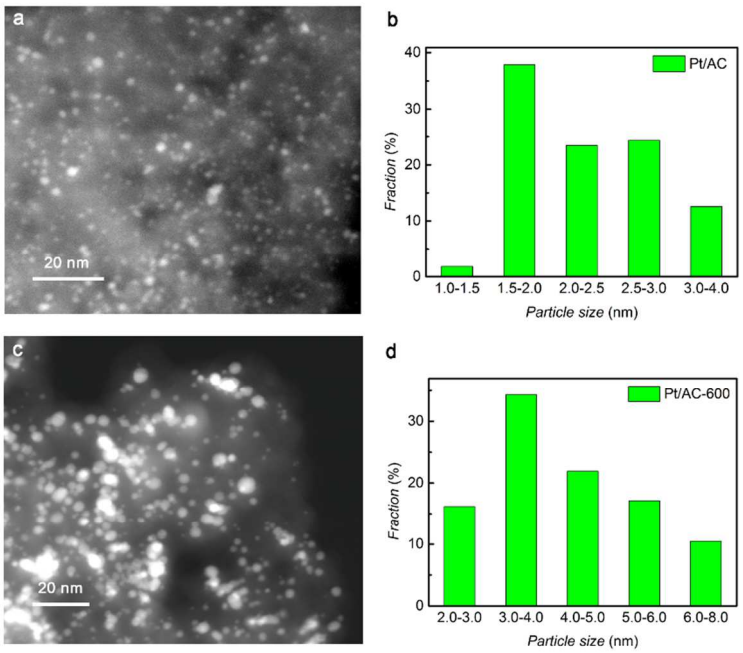

Figure S7. STEM images and Pt nanoparticle size distributions of (a, b) Pt/AC and (c, d) Pt/AC-600. '-600' represents the annealed catalysts. The theoretical Pt weight loading was 5 wt% for Pt/AC.

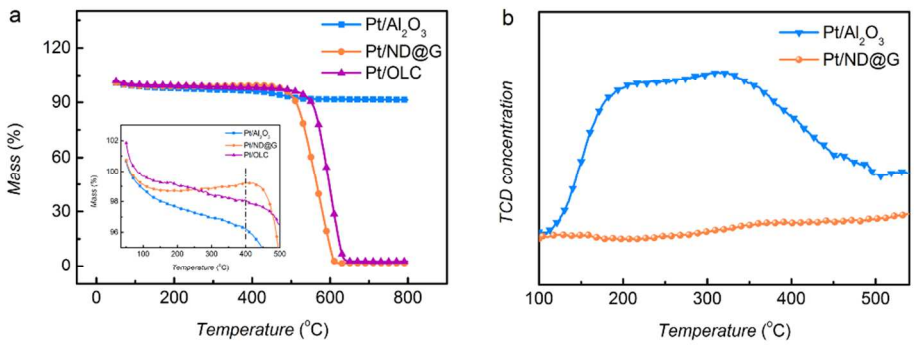

Figure S8. (a) TG-MS and (b) NH_3-TPD profiles of the as-prepared catalysts. The theoretical Pt weight loading for Pt/Al_2O_3 was 0.3 wt%, and those for Pt/ND@G and Pt/OLC were both 0.5 wt%.

It is well-known that nanodiamond is one of the nanocarbons. Higher temperature and oxygen content will lead to the combustion of the nanodiamond; in addition, there was a sharp decrease at approximately 500 ºC in the TG-MS profile of Pt/ND@G, which was due to the combustion of support and coke depositing on the support, and it is very difficult to distinguish the contribution of support and coke on the support based on the literatures; besides, coke on the support has small effect on the catalytic activity. Thus, the weight-loss above 400 °C was ignored.

Our previous work[7] found that the high initial activity of nanodiamond in the steam-free dehydrogenation of ethylbenzene reaction can be fully restored by flowing air through the sample at 400 ºC. Shi et al.[8] considered that the combustion of coke below 400 ºC was mainly the deposits covering the active metal, while the combustion at higher temperature attributed to the coke locating on the surface of the support for Pt/Al_2O_3 catalyst, which was in well agreement with the opinion of Martín et al.'s.[9] Thus, we consider the combustion of coke below 400 ºC as the deposits covering the active metal, while the combustion at higher temperature attributes to the support and coke locating on the surface of the support.

The amount of coke deposits covering Pt nanoparticles for Pt/Al_2O_3 (4.5 wt%) is approximately three times more than that for Pt/ND@G (1.5 wt%, Table 1 and Figure S8a). The acidities of the as-prepared catalysts were measured by NH_3-TPD technique.

There is few desorption peak for Pt/ND@G and the acidity of Pt/Al_2O_3 is stronger than that of Pt/ND@G (Figure S8b), in accordance with the result of Table S1. The ND@G support was obtained by calcining ND in N_2 atmosphere at 1100 ºC and most of the unstable oxygen containing groups would be desorbed. Therefore, the acidity of Pt/ND@G catalyst is weaker than Pt/Al_2O_3. Coke deposition is another main reason leading to the catalyst deactivation for PDH.[10] Lower acidity can decrease side-reactions such as polymerization and condensation, making the coke deposited on Pt/ND@G less than on Pt/Al_2O_3,[11] which helps to achieve higher stability for Pt/ND@G in harsh reaction conditions.

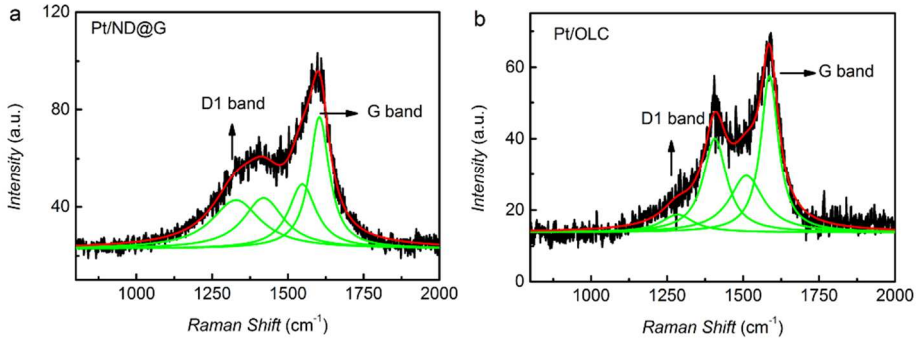

Figure S9. Raman spectra of the as-prepared catalysts. (a) Pt/ND@G and (b) Pt/OLC. The theoretical Pt weight loadings for Pt/ND@G and Pt/OLC were both 0.5 wt%.

Generally, there are five different fitted Raman spectra existed in ND samples in the range of 800-2000 cm^{-1}. D1 band located in ca. 1350 cm^{-1} represents the edge of graphite crystallite, D2 band appeared at ca. 1620 cm^{-1} contributes to the disordered graphite crystallite, D3 band located in ca. 1500 cm^{-1} is the amorphous carbon, D4 band located in ca. 1200 cm^{-1} attributes to the impurities on the carbon surface, and G band located in ca. 1580 cm^{-1} is assigned to the ideal graphite structure.[12] The intensity ratio of D1 and G bands (I_{D1}/I_G) was used to evaluate the degree of disorder for carbon materials, and higher I_{D1}/I_G indicates more defects in the catalyst system. There are more defects in Pt/ND@G (I_{D1}/I_G=0.91) than in Pt/OLC (I_{D1}/I_G=0.21) through fitting and calculating (Table 1).

Supporting References

(1) Parry, E. P. *J. Catal.* **1963**, *2*, 371-379.

(2) Ravenelle, R. M.; Copeland, J. R.; Kim, W. G.; Crittenden, J. C.; Sievers, C. *ACS Catal.* **2011**, *1*, 552-561.

(3) Liu, J.; Liu, C.; Ma, A.; Rong, J.; Da, Z.; Zheng, A.; Qin, L. *Appl. Surf. Sci.* **2016**, *368*, 233-240.

(4) Yu, C.; Xu, H.; Ge, Q.; Li, W. *J. Mol. Catal. A:- Chem.* **2007**, *266*, 80-87.

(5) Siri, G. J.; Ramallo-López, J. M.; Casella, M. L.; Fierro, J. L. G.; Requejo, F. G.; Ferretti, O. A. *Appl. Catal., A* **2005**, *278*, 239-249.

(6) Pisduangdaw, S.; Panpranot, J.; Methastidsook, C.; Chaisuk, C.; Faungnawakij, K.; Praserthdam, P.; Mekasuwandumrong, O. *Appl. Catal., A* **2009**, *370*, 1-6.

(7) Zhang, J.; Su, D.; Blume, R.; Schlögl, R.; Wang, R.; Yang, X.; Gajović, A. *Angew. Chem., Int. Ed.* **2010**, *49*, 8640-8644.

(8) Shi, L.; Deng, G.; Li, W.; Miao, S.; Wang, Q.; Zhang, W.; Lu, A. *Angew. Chem., Int. Ed.* **2015**, *54*, 13994-13998.

(9) Martín, N.; Viniegra, M.; Lima, E.; Espinosa, G. *Ind. Eng. Chem. Res.* **2004**, *43*, 1206-1210.

(10) Sattler, J. J. H. B.; Ruiz-Martinez, J.; Santillan-Jimenez, E.; Weckhuysen, B. M. *Chem. Rev.* **2014**, *114*, 10613-10653.

(11) Li, Q.; Sui, Z.; Zhou, X.; Zhu, Y.; Zhou, J.; Chen, D. *Top. Catal.* **2011**, *54*, 888-896.

(12)Su, D. In *Nanocarbon Catalysis*; Bai, C., Ed.; Science Press: Beijing, 2014, p 21-22.